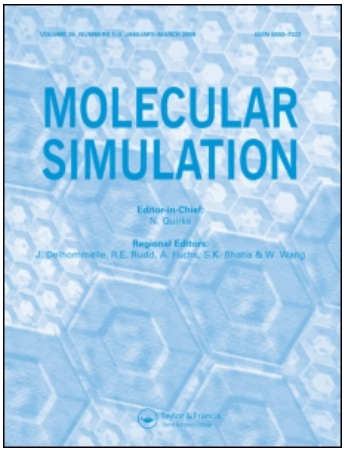

Molecular Simulation
Publication details, including instructions for authors and subscription information:
http://www.informaworld.com/smpp/title~content=t713644482

State point dependence of systematically coarse-grained potentials

Jayeeta Ghosh[a]; Roland Faller[a]
[a] Department of Chemical Engineering and Materials Science, Davis, CA, USA

To cite this Article Ghosh, Jayeeta and Faller, Roland(2007) 'State point dependence of systematically coarse-grained potentials', Molecular Simulation, 33: 9, 759 — 767
To link to this Article: DOI: 10.1080/08927020701275050
URL: http://dx.doi.org/10.1080/08927020701275050

Molecular Simulation, Vol. 33, Nos. 9–10, 15–30 August 2007, 759–767

Taylor & Francis
Taylor & Francis Group

State point dependence of systematically coarse–grained potentials

JAYEETA GHOSH and ROLAND FALLER*

Department of Chemical Engineering and Materials Science, UC Davis, Davis, CA 95616, USA

(Received December 2006; in final form February 2007)

We apply systematic structural coarse–graining based on optimizing a potential against the structure obtained in atomistic simulations to the small organic glass former ortho-terphenyl (OTP). Atomistic radial distributions at various temperatures ranging from below the glass transition temperature to the equilibrium liquid show hardly any change with temperature. These pair distribution functions are used as targets to be reproduced by a mesoscale model of OTP which is formulated by replacing each benzene ring with a single interaction center. The potentials are obtained by Iterative Boltzmann Inversion of the distribution functions. The resulting potential depends not only on the structure but also implicitly on the temperature at which it was optimized. Potentials optimized in the liquid range lead to crystalline structures if used below the glass transition requiring independent optimizations in the glass. We compare potentials optimized in both ranges to study the system over the whole temperature range. The dynamic mapping turns out to be different for different mapping potentials.

Keywords: Molecular dynamics; Coarse–graining; Multiscale modeling; Glasses; Ortho-terphenyl; Iterative Boltzmann inversion

1. Introduction

A liquid, which does not crystallize on cooling, undergoes a "glass transition", a falling-out-of equilibrium in terms of motion and rearrangement of its constituents [1,2]. The rapid increase in viscosity near the glass transition temperature, T_g, transforms the liquid into a solid lacking crystal order. This glass transition is associated with structural and dynamic anomalies and has been the subject of extensive thermodynamic, kinetic and structural investigation and modeling at the molecular level. A particularly well studied example of a so-called glass former is ortho-terphenyl (OTP) [3–12]. It has for a simulation study also the advantage that it is a small molecule limiting simulation time. In this contribution we show the challenges the glass transition poses in simulations even for a small molecule like OTP. Very low temperature simulations even of simple model glasses have generally been avoided, and extrapolations are routinely used to infer low temperature behavior [13–16]. This stems from the fact that simulations near or even below a glass transition are notoriously difficult, and the results must be considered with caution. The relevant time scales below T_g are too long to be sampled by conventional molecular simulation. In order to address fundamental questions of glasses, we require advanced molecular simulation techniques. One such approach which has gained significant momentum over recent years is structural coarse–graining [17–27].

In any simulation (atomistic or meso-scale), as in any experiment, one must first define the system being studied. In the case of coarse–graining or multi-scale modeling we must consider the different models that can be used and their relationship to each other. We use here a technique which is based on standard atomistic modeling to develop the meso-scale system. In a meso-scale model a group of atoms is often replaced by a single interaction center which we here call a super-atom. The super-atoms are the only interaction centers in a meso-scale simulation and indirectly carry the information of the interactions between the real atoms in their local geometrical arrangements. The choice of which super-atoms to use is arbitrary in principal, but there exist a number of criteria to consider when making this selection [27].

*Corresponding author. Email: rfaller@ucdavis.edu

Molecular Simulation
ISSN 0892-7022 print/ISSN 1029-0435 online © 2007 Taylor & Francis
http://www.tandf.co.uk/journals
DOI: 10.1080/08927020701275050

2. Structural coarse–graining

2.1 Iterative Boltzmann inversion

In detailed atomistic simulations distributions of bond lengths, bond angles, torsions as well as the radial distribution function can be recorded between pre-defined super-atoms. The subsequent meso-scale simulation has to be designed in order to reproduce these distributions. If we achieve that we can meaningfully say that the meso-scale simulation and the atomistic model represent the same system. The most efficient (canonical) way to obtain an effective potential from a sampled distribution is the Boltzmann inversion. The distributions have to be normalized by the Jacobian between spherical and Cartesian coordinates [18]. Formally, the Boltzmann inversion leads to a free energy difference which only in infinite dilution and for a homogeneous one-component system would equal the potential energy

$$V(\zeta) = -k_B T \ln p(\zeta) \tag{1}$$

where k_B is the Boltzmann constant, T is temperature and p is a probability distribution function. Here ζ can stand for bond lengths, bond angles and torsions alike. It is noteworthy that this potential is completely numerical. If we, e.g., start from the atomistic radial distribution function $g_{at}(r)$, where r is the distance, we obtain a potential of mean force which is the initial guess of the potential

$$V_0(r) = F(r) = -k_B T \ln g_{at}(r). \tag{2}$$

Simulation of a system using this initial potential yields a corresponding $g_0(r)$, which is different from the atomistic target result $g_{at}(r)$ as it includes packing effects which depend on temperature. The potential needs to be improved, which can be done by a correction term $-k_B T \ln(g_0(r)/g_{at}(r))$ leading to the iterative cycle as follows:

$$V_{i+1}(r) = V_i(r) - w_i(r) k_B T \ln(g_i(r)/g_{at}(r)). \tag{3}$$

where $w_i(r)$ can be a weighting function corresponding to the i-th cycle and $g_i(r)$ and $V_i(r)$ are radial distribution function and potential, respectively, for that cycle. The weighting function is used to focus on specific parts of the structure more strongly. This procedure is iterated until the coarse–grained model and the atomistic model coincide. From 10 to 15 iterations have been necessary for OTP at different temperatures. For polymers or other larger molecules typically 25–40 iterations are required making this a time consuming but highly accurate technique [22,24].

2.2 State point dependence of the potentials

It is clear from the nature of the optimization that all structurally coarse–grained models are developed using a single state point. So the concentration and temperature dependence of the developed meso-scale models has to be determined. As different local conformations in the atomistic system enter the coarse–graining at different state points, coarse–grained models are dependent on the thermodynamic state. A goal is, therefore, to develop a model which can be used for a wide range of temperatures and compositions. For this purpose, the Iterative Boltzmann Inversion method [19] will here be critically assessed in how far a potential can be used at a state point it has not been optimized for. Recently, we reported preliminary results on the temperature dependence of a polystyrene model and found that the coarse–grained model shows a much too strong dependence on temperature [10]. Other groups found such problems as well [28]. It has been shown that the resulting potentials are thermodynamically consistent in the sense that at the given state point the thermodynamics is correct even if we only use the radial distribution function as target as the resulting potential is unique [26,29]. The addition of pressure corrections or similar may speed up the algorithm but does not fundamentally improve it.

3. Application of the Iterative Boltzmann inversion to the organic glass former ortho-terphenyl

3.1 Atomistic simulations of ortho-terphenyl

Ortho-terphenyl is a small organic glass former and an ideal model system to study the glass transition [11,12]. The molecule consists of three benzene rings with two rings in ortho positions of the central one. We perform atomistic molecular dynamics simulations using GROMACS v3.2 [30]. Although simple in structure devising a well-suited computer model for OTP is challenging. We need an atomistic model to study inter-molecular as well as intra-molecular motions. For dynamical studies we need a simple model. Our atomistic OTP model which we use as a starting point for the optimization bases on the model by Kudchadkar *et al.* [9]. It includes one united atom site for each carbon with its corresponding hydrogen if present. We fix C—C bond lengths to 0.141 nm using LINCS and use a harmonic angle potential of $500\,\mathrm{kJ\,mol^{-1}\,rad^{-2}}$ to keep 120° between C—C—C. The benzene rings are kept planar by an improper dihedral. A Lennard–Jones potential with $\epsilon = 55.3\,\mathrm{K}$ and $\sigma = 3.72\,\text{Å}$ issue with unit ε is used where the parameters have been developed for benzene [9]. We model torsions by repulsive Lennard–Jones interactions between the outer rings fitted against experiments. Simulation details of the atomistic simulations are reported in [12]. Our OTP system consists of 800 molecules in a cubic box under periodic boundary conditions with a 2 fs time step in the *NPT* ensemble. The system was studied at 11 different temperatures from below the glass transition temperature to well above. From the density vs. temperature plot as shown in figure 1(a) we found the glass transition temperature to be around 260 K compared to the experimental value of 243 K [3,6]. We show in figure 1(b) the atomistic radial distribution

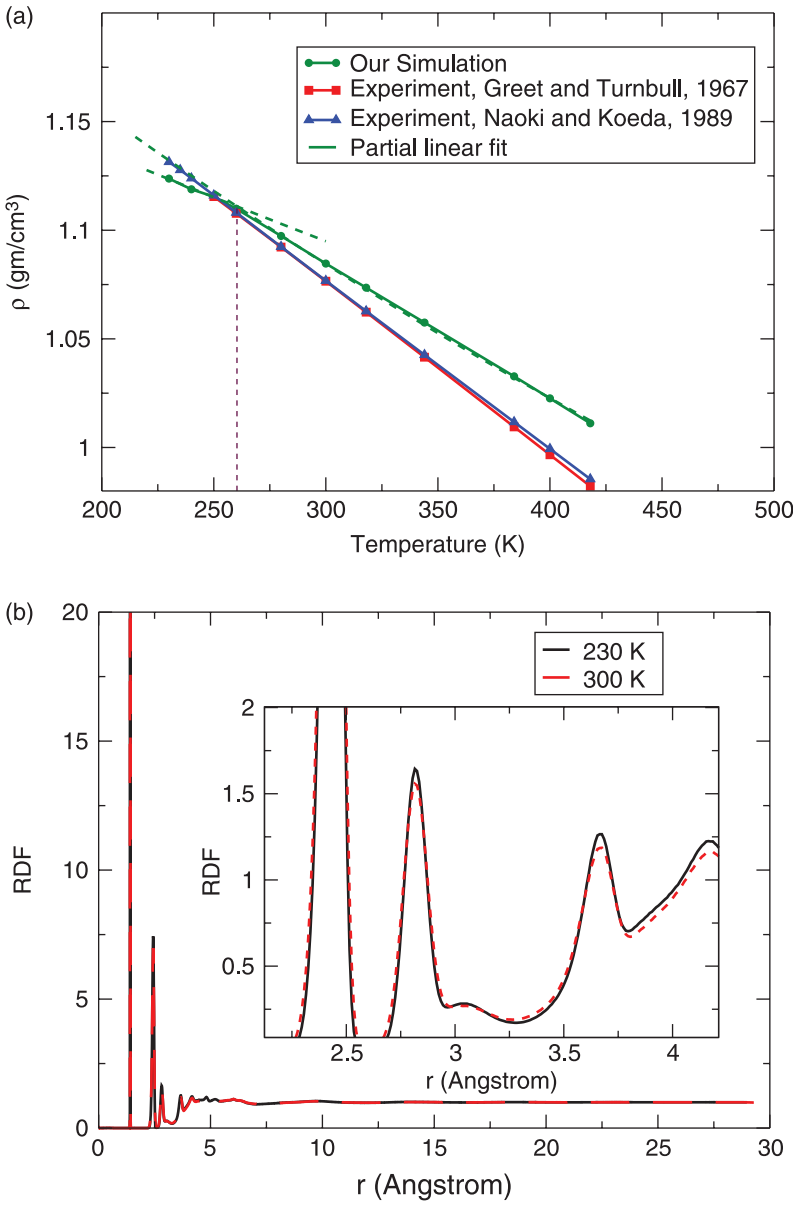

Figure 1. Results from atomistic simulation. (a) Density vs. temperature plot compared with experimental results. (b) Comparison of radial distribution functions at 230 K (solid-line) and 300 K (dashed-line). Part of the plot is zoomed in the inset of the figure for better comparison.

function of the whole molecule at 230 and 300 K. The radial distribution functions show very little variation with temperature as depicted from the figure. This leads us to the initial assumption that the coarse–grained model should be only very weakly temperature dependent. This will turn out to be incorrect.

3.2 Implementation of a meso-scale model of ortho-terphenyl

In the meso-scale model of ortho-terphenyl each benzene ring is replaced by a single interaction center (a super-atom) as shown in figure 2 [11]. It satisfies the basic requirements [27] that the distances between bonded super-atoms follow well-defined single peak distributions. The single peak distribution is modeled by a single Gaussian curve, which defines a harmonic bond potential. Our meso-scale model does not use angle, dihedral or tethering potentials. We instead use a fictitious bond potential between the outer rings to model the coarse–grained angle. Cross dependencies between different potentials are neglected. For the non-bonded potential we use the Iterative Boltzmann Inversion described above. OTP is modeled as a trimer of type 1–2–1. This means that the two outer rings are required to have the same interaction. This leads to three interdependent radial distribution functions to be optimized [31]. We cannot assume any mixing rules *a priori*. Radial distribution functions from different iteration cycles during the optimization at different temperatures are shown in figures 3 and 4 for 230 and 300 K, respectively. The rdfs are compared with the atomistic center of mass radial

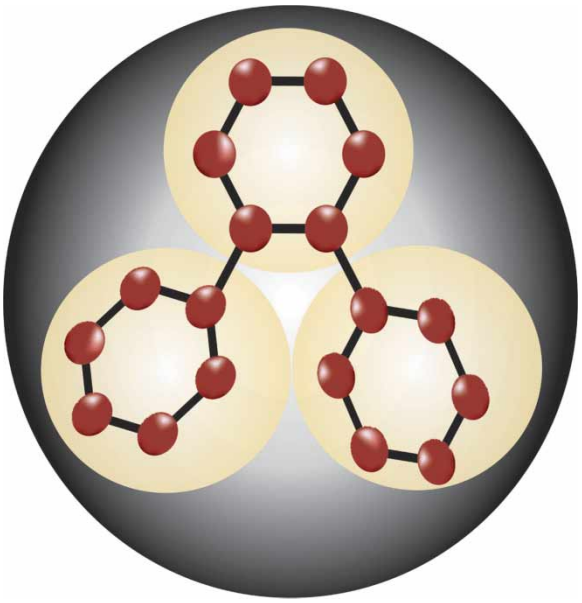

Figure 2. Ortho-terphenyl and the mapping into the meso-scale model.

distribution functions (solid lines in figures 3 and 4) of corresponding temperatures for specific interactions. Iteration was deemed converged until all coarse–grained rdfs were within 5% of the atomistic target, i.e. the maximum difference was not larger than 5% of the target value. The optimization was performed independently at temperatures in the glassy (230 K) and liquid region (300 K). In every iteration we ensured that the simulation is equilibrated by monitoring the dependence of the radial distribution function on simulation time. We use the DLPOLY [32,33] molecular dynamics simulation package for the meso-scale simulations. We took the final configuration from the atomistic simulation at 300 K to initialize the meso-scale simulation with 800 OTPs. The meso-scale simulations have been performed under *NVT* conditions at the density which is equal to the density of atomistic simulation at 300 K (1084 kg/m^3).

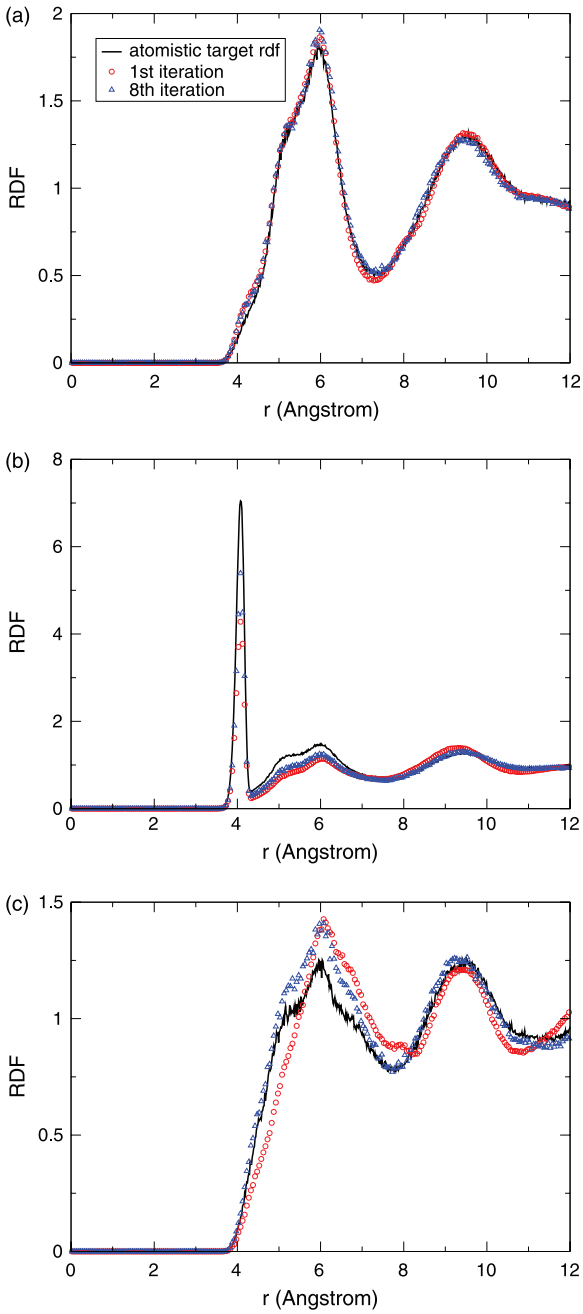

Figure 3. Radial distribution functions from iterative Boltzmann inversion cycles at 230 K. (a) 1–1 interaction, (b) 1–2 interaction, and (c) 2–2 interaction. Interaction center 1 corresponds to the outer ring sites and 2 to the central ring sites.

4. Results and discussion

4.1 Comparison of potentials obtained at different temperatures

We performed simulations over a range of temperatures with the potential optimized at 300 K, i.e., the liquid range potential. The immediate result was that the system does not form a glass but crystallizes. So an additional iteration was performed at 230 K in the glassy range and the application of the resulting potential in the glassy range led to formation of glasses at lower temperatures. Figure 5(a) shows the snapshot of the crystal structure at 230 K using liquid range (300 K) potential whereas figure 5(b) shows the glassy structure at the same temperature using the glassy range (230 K) potential. It is not easy to define a glass transition temperature using the coarse–grained model as there is an ambiguity up to which point we should use the liquid potential and where to use the glassy potential. A canonical solution would be to optimize a coarse–grained potential at every single state point but that obviously defeats the purpose of the coarse–graining. The glass transition temperature will clearly vary between the meso-scale model and the atomistic model as well as between different meso-scale models. We do not see any transition, formation of crystal or glass, at temperatures of 250 K or above for the meso-scale

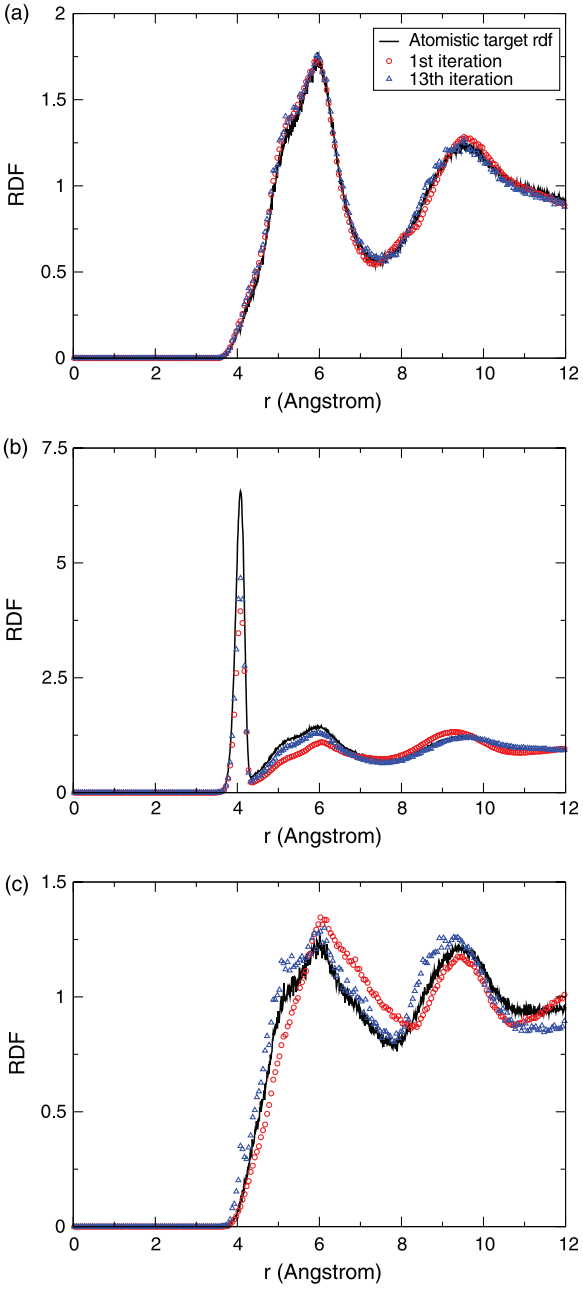

Figure 4. Iterative Boltzmann inversion cycles at 300 K. Subfigures as defined in figure 3.

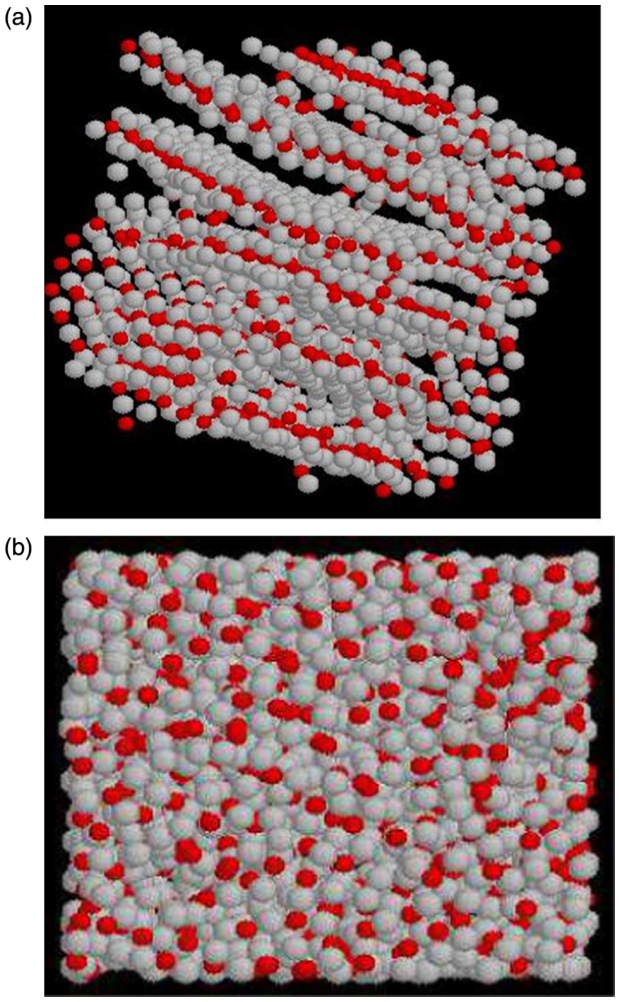

Figure 5. Snapshots of the system at 230 K. (a) Using the 300 K potential we see formation of a crystal. (b) Using the 230 K potential we find a glassy structure.

model developed at 300 K compared to the glass formation in the atomistic model at 260 K.

Radial distribution functions at 230 K (figure 6) show clear evidence of crystal formation instead of glass for the 300 K developed potential. This crystallization tendency has been found for polymeric glass-forming systems as well [10]. In figure 7 we show the resulting potential as obtained by iterative Boltzmann inversion of the atomistic radial distribution functions at 230 and 300 K. The radial distribution functions depend only weakly on temperature; but the inversion process itself depends explicitly on temperature which leads to a significant change in potential even if the radial distribution functions themselves are extremely similar. Even if they were identical the potential would be different. Conversely in the typical case of a temperature independent potential, as assumed in an atomistic simulation, the structure is temperature dependent.

We carried out direct simulations using both potentials in the transition temperature region as determined by the atomistic simulation between the liquid and the glass at 260 K. In figure 8 we show the rdfs from both runs in comparison to the atomistic rdf as determined at 260 K. Here the high temperature optimized potential does not show a crystallization yet. Still, we already see that the potential from 300 K leads to overly pronounced structures, whereas the lower temperature optimization leads to a realistic representation of the 260 K atomistic data. This is understandable as the atomistic rdfs are very similar for OTP; the higher temperature leads to a more pronounced potential. This depends on the following: Consider two points in distance r_1 and r_2 where $g(r_1) > g(r_2)$ and for simplicity we assume that the rdfs are identical. Correspondingly, we can expect from the Boltzmann inversion that $V(r_1) < V(r_2)$. If we now assume that we do

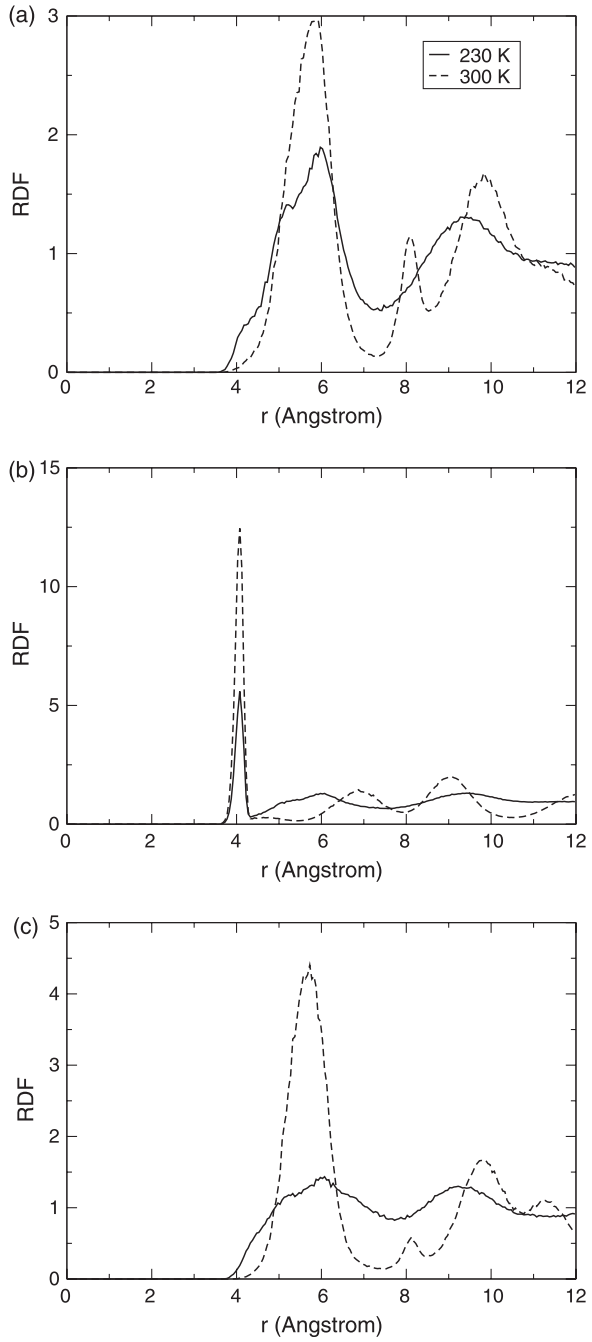

Figure 6. Radial distribution function at 230 K for different combination of rings, optimized at 230 and 300 K. The dashed lines (using the 300 K potential) represents the formation of a crystal structure compared to the solid lines (230 K potential).

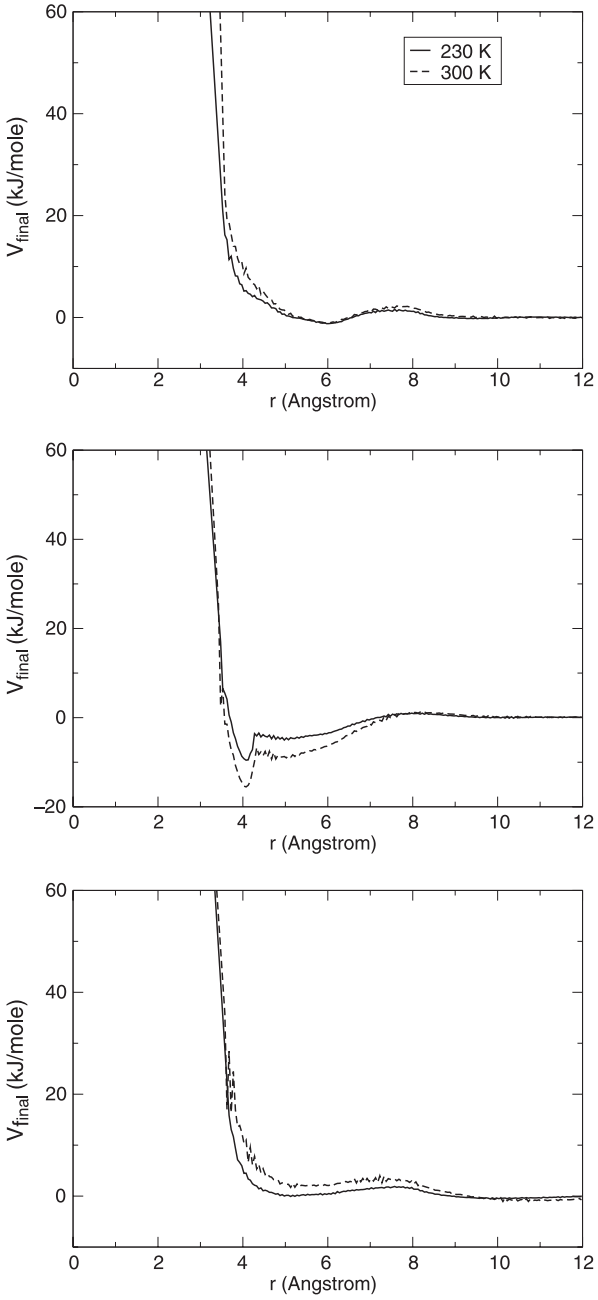

Figure 7. Optimized potential for different combination of rings optimized at 230 and 300 K: (a) Ring 1–Ring 1, (b) Ring 1–Ring 2, and (c) Ring 2–Ring 2.

not need to iterate—often the direct inversion gives a reasonable approximation of the final potential—we see that $V(r_2) - V(r_1) = k_B T \ln g(r_2)/g(r_1)$. Thus the potential differences scale in first approximation with the temperature at which the iteration is performed for the same rdf.

4.2 Dynamic mapping

Our atomistic simulations as most molecular dynamics simulations utilize a 2 fs time-step which is required to be about an order of magnitude smaller than the fastest characteristic time which here involve bond angle vibrations on the order of tens of femtoseconds. With a reasonable use of computer resources one can reach into the nanosecond time-range. Structural mapping techniques lead inherently to larger time-scales because the fastest degrees of freedom are now bonded motions of super-atoms. As dynamic investigations are often desired one must find a correct mapping of the time-scales involved in the different models. We are using diffusion coefficients for calibrating the time-scale. For long enough simulations any molecule will end up in diffusive motion

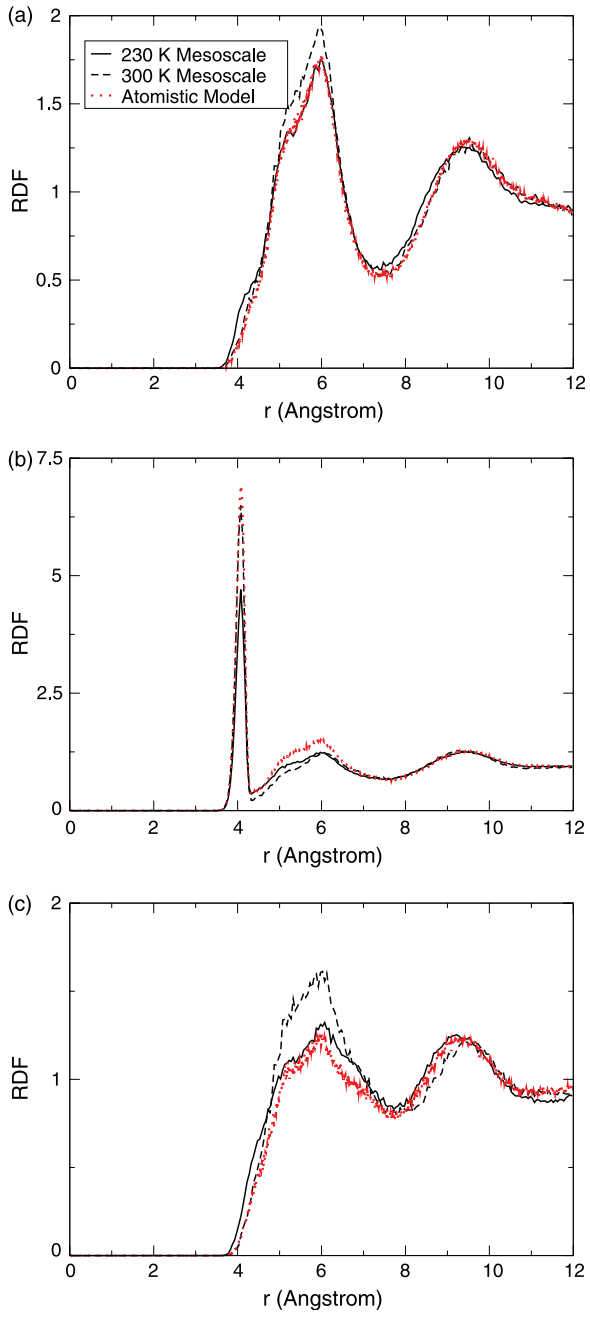

Figure 8. RDFs at 260 K using 230 and 300 K potentials. Subfigures as defined in figure 3.

if all internal degrees of freedom are relaxed. The static mapping leads to the mapping of length scales through the above described radial distribution functions. Now the two diffusion coefficients can be equated and the time scale is fixed. Diffusion coefficients in simulations can be determined by the mean-square displacement through the Einstein relation

$$D = \frac{1}{2d} \lim_{\Delta t \to \infty} \frac{\langle (x(t + \Delta t) - x(t))^2 \rangle}{\Delta t} \qquad (4)$$

where d is the dimensionality of the system and $x(t)$ is the position of the corresponding particle at time t. We have to note here that we compare diffusion coefficients in the NVT and NpT ensemble where we fundamentally would expect some differences [34]. However, as we stay within one ensemble for all atomistic and all coarse–grained runs we can neglect this effect.

In figure 9 we show the mean square displacement of meso-scale OTP at various temperatures. Here, we used the liquid model optimized at 300 K for simulations of 250 K and above and the glass model, optimized at 230 K for the two lowest temperatures in order to circumvent the crystallization. Figure 9(a) shows uncorrected MSDs before any specific dynamic mapping. From the figure the glassy OTP (230 and 240 K) seems to be more mobile than the low temperature liquid, which is misleading conceptually. We have to be very careful about comparing the results coming out of two different potentials. To really compare the mobility we calculated the diffusivity using both meso-scale potentials and compared with the atomistic data at every temperature and matched the timescale as described above. The mean square displacement as found after dynamic mapping is shown in figure 9(b) which shows the correct order of temperatures. Here, all simulations using the 230 K model are scaled by a factor of 31.06 and the simulations using the 300 K model are scaled by a factor of 6.905. These factors have been determined by mapping of the dynamics at the temperatures at which the meso-scale models have been developed. This shows that the effective speedup depends on the degree of coarse–graining. In figure 9(c) we show how the mean-squared displacements look like if every individual simulation is mapped by a different scaling factor to the atomistic simulation. Still, the simulations shown by the dashed lines are performed using the 230 K model and the other ones by the 300 K model. The corresponding scaling factors are found in Table 1. We find that using a single scaling factor for every model yields a qualitatively correct dynamic mapping. However, in order to obtain quantitative data every simulation has to be mapped independently. In our temperature range we have otherwise errors on the order of a factor 2–3. If we compare figure 9(b),(c) we see that by individual mapping all the lowest temperatures behave very similarly which is expected in the glassy range.

Table 1. Scaling factors for dynamic mapping at different temperatures.

Temperature (K)	*Scaling factor*
230	31.06
240	42.62
250	11.43
260	12.96
280	10.61
300	6.91
318	4.84
344	3.95
384	2.78
400	2.32
418	2.40

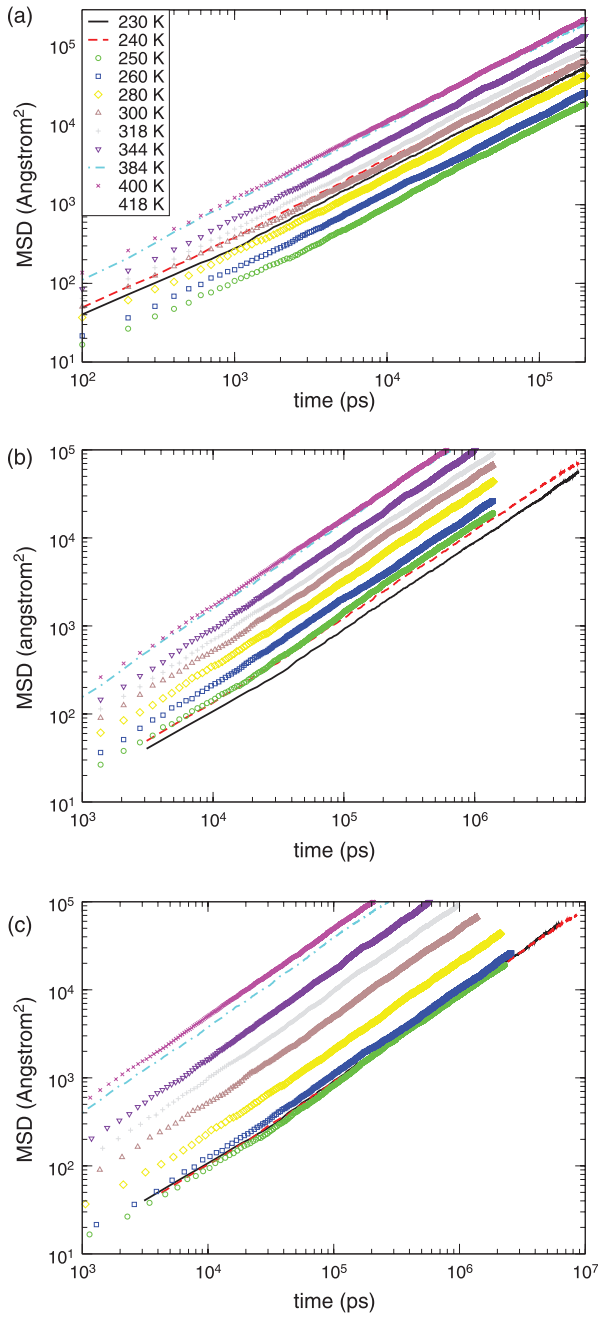

Figure 9. Mean square displacement before (a) and after dynamic mapping (b, c) (see text) on double logarithmic scale.

5. Conclusions

We have clearly shown that structurally coarse–grained potentials are extremely susceptible to artifacts if we use them outside the temperature region for which they were optimized. The results here focus on ortho-terphenyl but results on polystyrene [10] and polyethylene [28] suggest that is a general problem. There is fundamentally no way out of this dilemma at least using pair potentials as Henderson's theorem [29] shows that any pair potential leading to the same structure is identical meaning that structural coarse–graining has one single solution for a given structure.

We have used temperature as an example here but we expect that, e.g. concentration effects will lead to the same problems. Preliminary results with mixed polymer systems show that there is a significant effect of concentration on the optimized potential.

Additionally, we have to be very careful in the interpretation of timescales deduced from meso-scale simulations as we see that even if the structure at another temperature is acceptable using a meso-scale model we can not assume that the timescale is temperature independent.

All these findings are not meant to dissuade from the use of systematic multiscale techniques. There is no alternative to them. But one has to be very careful in their use especially over a range of conditions.

One possibility to improve the coarse–grained results is to perform coarse–grained *NpT* simulations and compare with the atomistic simulations. It may well be the case that the density effects are at least partially canceling temperature effects.

Acknowledgements

This work was supported by the US Department of Energy, Office of Science, Office of Advanced Scientific Computing Research under Grant No. DE-FG02-03ER25568. This research also used resources of the National Energy Research Scientific Computing Center, which is supported by the Office of Science of the US Department of Energy under Contract No. DE-AC03-76SF00098.

References

[1] M.D. Ediger, C.A. Angell, S.R. Nagel. Supercooled liquids and glasses. *J. Phys. Chem.*, **100**, 13200 (1996).
[2] P.G. Debenedetti, F.H. Stillinger. Supercooled liquids and the glass transition. *Nature*, **410**, 259 (2001).
[3] R.J. Greet, D. Turnbull. Glass transition in *o*-terphenyl. *J. Chem. Phys.*, **46**, 1243 (1967).
[4] D.W. McCall, D.C. Douglass, D.R. Falcone. Molecular motion in ortho-terphenyl. *J. Chem. Phys.*, **50**, 3839 (1969).
[5] S.S. Chang, A.B. Bestul. Heat capacity and thermodynamic properties of *o*-terphenyl crystal, glass, and liquid. *J. Chem. Phys.*, **56**, 503 (1972).
[6] M. Naoki, S. Koeda. Pressure–volume–temperature relations of liquid, crystal, and glass of *o*-terphenyl. Excess amorphous entropies and factors determining molecular mobility. *J. Phys. Chem.*, **93**, 948 (1989).
[7] G. Baranovic, L. Bistricic, V. Volovsek, D. Kirin. Molecular vibrations and lattice dynamics of ortho-terphenyl. *Mol. Phys.*, **99**, 33 (2001).
[8] R.J. Berry, D. Rigby, D. Duan, M. Schwartz. Molecular dynamics study of translational and rotational diffusion in liquid ortho-terphenyl. *J. Phys. Chem. A*, **110**, 13 (2006).
[9] S.R. Kudchadkar, J.M. Wiest. Molecular dynamics simulations of the glass former ortho-terphenyl. *J. Chem. Phys.*, **103**, 8566 (1995).
[10] J. Ghosh, B.Y. Wong, Q. Sun, F.R. Pon, R. Faller. Simulations of glasses: multiscale modeling and density of states Monte Carlo simulations. *Mol. Simul.*, **32**, 175 (2006).

[11] J. Ghosh, R. Faller. Modelling of the glass transition of ortho-terphenyl in bulk and thin films. In *Mechanics of Nanoscale Materials and Devices*, vol. 924E of *Mater. Res. Soc. Symp. Proc.* A. Misra, J. Sullivan, H. Huang, K. Lu, S. Asif (Eds.), p. 0924-Z03-21, MRS, Warrendale, PA (2006).
[12] J. Ghosh, R. Faller. A comparative molecular simulation study of the glass former ortho-terphenyl in bulk and free standing films. *J. Chem. Phys.*, **125**, 044506 (2006).
[13] S. Büchner, A. Heuer. Potential energy landscape of a model glass former: thermodynamics, anharmonicities, and finite size effects. *Phys. Rev. E*, **60**, 6507 (1999).
[14] B. Coluzzi, G. Parisi, P. Verrocchio. Thermodynamical liquid–glass transition in a Lennard–Jones binary mixture. *Phys. Rev. Lett.*, **84**, 306 (2000).
[15] B. Coluzzi, G. Parisi, P. Verocchio. Lennard–Jones binary mixture: a thermodynamical approach to glass transition. *J. Chem. Phys.*, **112**, 2933 (2000).
[16] F. Sciortino, W. Kob, P. Tartaglia. Thermodynamics of supercooled liquids in the inherent-structure formalism: a case study. *J. Phys.: Condens. Matter*, **12**, 6525 (2000).
[17] A.P. Lyubartsev, A. Laaksonen. A calculation of effective interaction potentials from radial-distribution functions: a reverse Monte Carlo approach. *Phys. Rev. E*, **52**, 3730 (1995).
[18] W. Tschöp, K. Kremer, J. Batoulis, T. Bürger, O. Hahn. Simulation of polymer melts. I. Coarse–graining procedure for polycarbonates. *Acta Polym.*, **49**, 61 (1998).
[19] D. Reith, M. Pütz, F. Müller-Plathe. Deriving effective meso-scale coarse graining potentials from atomistic simulations. *J. Comput. Chem.*, **24**, 1624 (2003).
[20] F. Müller-Plathe. Coarse–graining in polymer simulation: from the atomistic to the meso-scopic scale and back. *Chem. Phys. Chem.*, **3**, 754 (2002).
[21] F. Müller-Plathe. Scale-hopping in computer simulations of polymers. *Soft Mater.*, **1**, 1 (2003).
[22] R. Faller, D. Reith. Properties of polyisoprene—model building in the melt and in solution. *Macromolecules*, **36**, 5406 (2003).
[23] R. Faller. Correlation of static and dynamic in homogeneities in polymer mixtures: a computer simulation of polyisoprene and polystyrene. *Macromolecules*, **37**, 1095 (2004).
[24] Q. Sun, R. Faller. Systematic coarse–graining of atomistic models for simulation of polymeric systems. *Comput. Chem. Eng.*, **29**, 2380 (2005).
[25] Q. Sun, R. Faller. Crossover from unentangled to entangled dynamics in a systematically coarse–grained polystyrene melt. *Macromolecules*, **39**, 812 (2006).
[26] S. Jain, S. Garde, S.K. Kumar. Do inverse Monte Carlo algorithms yield thermodynamically consistent interaction potentials? *Ind. Eng. Chem. Res.*, **45**, 5614 (2006).
[27] R. Faller. Coarse–grain modeling of polymers. In *Reviews in Computational Chemistry*, K. Lipkowitz, T. Cundari, D. Boyd (Eds.), vol. 23, chap. 4 Wiley-VCH, New York (2007).
[28] T. Vettorel, H. Meyer. Coarse graining of short polyethylene chains for studying polymer crystallization. *J. Chem. Theor. Comp.*, **2**, 616 (2006).
[29] R.L. Henderson. Uniqueness theorem for fluid pair correlation-functions. *Phys. Lett. A*, **49**, 197 (1974).
[30] E. Lindahl, B. Hess, D. van der Spoel. Gromacs 3.0: a package for molecular simulation and trajectory analysis. *J. Mol. Model.*, **7**, 306 (2001).
[31] Q. Sun, R. Faller. Systematic coarse–graining of a polymer blend: polyisoprene and polystyrene. *J. Chem. Theor. Comp.*, **2**, 607 (2006).
[32] W. Smith, T. Forester. *J. Mol. Graphics*, 14 (1996).
[33] W. Smith, T. Forrester. The DLPOLY2 user manual. Tech. rep., Daresbury Lab (1999)
[34] H. Schmitz, R. Faller, F. Müller-Plathe. Molecular mobility in cyclic hydrocarbons: a simulation study. *J. Phys. Chem. B*, **103**, 9731 (1999).